Supplementary matrials for:

Filament Assembly by Spire: Key Residues and Concerted Actin Binding

Amy S. Rasson, Justin S. Bois, Duy Stephen L. Pham, Haneul Yoo, Margot E. Quinlan

Supplemental methods: protein purification

All constructs were transformed into *E. coli* BL21(DE3) cells (New England Biolabs, Ipswich, MA), and cultured in 1L TB media until an OD_{600} of 0.8 was reached. Expression was induced by adding 150-250 µM isopropyl-β-D-thiogalactopyranoside (IPTG). Cells transformed with single WH2-containing constructs shook for 18-20 h at 18°C post induction. Cells expressing WH2-Linker 3-WH2 constructs shook for 3 h at 37°C. Cells were harvested by centrifugation, pellets were resuspended in 15 mL of PBS (10 mM Na_2HPO_4, 1.8 mM KH_2PO_4, 140 mM NaCl, 2.7 mM KCl, pH 7.0), and centrifuged again before they were flash frozen and stored at −80°C.

Thawed cell pellets were resuspended in lysis buffer (PBS supplemented with 1 mM dithiothreitol (DTT), 1.7 mM phenylmethanesulfonyl fluoride (PMSF) and 1 µg/ml DNaseI. All subsequent steps were carried out at 4°C or on ice. Cells were lysed by two passages through a microfluidizer (Microfluidics, Newton, MA). The lysate was centrifuged at 20,000 $\times g$ for 20 min, and the supernatant was rocked with 1.5 mL glutathione-Sepharose 4b resin (GE Healthcare) for 1 h. Eluate was dialyzed in PBS supplemented with 1 mM DTT for 2 h at 4°C before the constructs were cleaved from GST by incubating them with 1-5% (w/v) PreScission protease overnight at 4°C. Both protease and cleaved GST were removed by rocking with fresh glutathione-Sepharose 4b resin for 1 h. The unbound fraction from the glutathione-Sepharose 4b resin was then dialyzed against 10 mM Tris pH 8.0, 100 mM KCl, and 1mM DTT, and further purified through anion exchange (MonoQ, GE Healthcare) by collecting the flow through. Fractions were pooled together and dialyzed against 10mM Tris pH 8.0, and 1mM DTT overnight at 4°C. Protein aliquots were flash-frozen in liquid nitrogen and stored at −80°C.

Due to a tendency to degrade, Sc and Sc[qe] were purified and frozen in one day. Modifications to this purification method were made for constructs that contained a His-tag (see Figure S1) in that these constructs were isolated from the cleaved GST and protease via TALON purification (Clontech, Mountain View, CA). All multiple WH2 domain-containing constructs were dialyzed into 20 mM HEPES pH 8.0, 100 mM KCl, and 1mM DTT, and further purified through cation exchange (MonoS, GE Life Sciences). Individual WH2 constructs were further purified through anion exchange as above. We were unable to purify Sa;, therefore it was synthesized by Biomatik USA, LLC.

Consideration of Sc/G-actin binding stoichiometry

The predicted SSPT curves for Sc do not match experimental measurements. In the main text, we posited that binding Sc to filaments can account for this discrepancy. Another possible explanation is that Sc may bind monomeric actin in two locations (which we shall call the two-site binding model). We explore this possibility here, looking first at the competition anisotropy assay.

The competition anisotropy data in the main text were fit with the titration curve resulting from

the following set of chemical reactions.

$$\mathrm{A}\cdot\mathrm{SD}^* \rightleftharpoons \mathrm{A} + \mathrm{SD}^* \qquad K_\mathrm{d}^* \tag{S1}$$

$$\mathrm{A}\cdot\mathrm{SC} \rightleftharpoons \mathrm{A} + \mathrm{SC} \qquad K_\mathrm{d}, \tag{S2}$$

where SD* denotes a fluorescently labeled SD domain. If we have a second binding site, we need also to consider the reactions

$$\mathrm{SC}\cdot\mathrm{A}\cdot\mathrm{SD}^* \rightleftharpoons \mathrm{SC} + \mathrm{A}\cdot\mathrm{SD}^* \qquad K_{\mathrm{d},12}^* \tag{S3}$$

$$\mathrm{SC}\cdot\mathrm{A} \rightleftharpoons \mathrm{SC} + \mathrm{A} \qquad K_{\mathrm{d},2} \tag{S4}$$

$$\mathrm{SC}\cdot\mathrm{A}\cdot\mathrm{SC} \rightleftharpoons \mathrm{SC} + \mathrm{A}\cdot\mathrm{SC} \qquad K_{\mathrm{d},12}. \tag{S5}$$

The fluorescence anisotropy signal r is given by

$$r = \frac{1}{c_{\mathrm{d}^*}^0}\left(r_f c_{\mathrm{d}^*} + r_1 c_{\mathrm{ad}^*} + r_2 c_{\mathrm{cad}^*}\right), \tag{S6}$$

where the notation for the concentrations of the respective species is intuitive. Given c_a^0, $c_{\mathrm{d}^*}^0$, and c_c^0, we can use EQTK to compute r. We have seven free parameters, r_f, r_1, r_2, and the four dissociation constants involving SC. In the absence of cooperative interactions between the two binding sites, we have $K_{\mathrm{d},2} \approx K_{\mathrm{d},12} \approx K_{\mathrm{d},12}^*$. We further assume that because the SC domain is much smaller than monomeric actin, $r_1 \approx r_2$. With these assumptions, we have four free parameters. Two of them, r_f and $r_b \equiv r_1 = r_2$ set the scale of the y-axis, while the dissociation constants K_d and $K_{\mathrm{d},2} = K_{\mathrm{d},12} = K_{\mathrm{d},12}^*$ set the shape of the curve.

We performed nonlinear regressions of the SC competition anisotropy curves using EQTK. The results are shown in Fig. S4C, along with the regression results from the one-site binding model. The results of the regression are shown in Table S1. We see that regressions of both models describe the experimental data well. Performing a hypothesis test on each regression suggests that the one-site binding model is more probable by a factor of 1.6, 4.5, and 56.4, for the blue, red, and green curves, respectively.

Table S1: **Competition anisotropy results for SC**

model	$\Delta_r G$ (kJ/mol)	$\Delta_r G_2$ (kJ/mol)	K_d (µM)	$K_{\mathrm{d},2}$ (µM)
one-site	3.88±0.24	—	0.21	—
two-site	5.40±0.11	1.22±0.08	0.11	0.61

While the one-site model is more probable from the competition anisotropy assays, it fails to describe the SSPT curves. Referring to Figure 7 in the main text, the corner concentration predicted by the one-site binding model in the absence of filament binding is too small to match the experimental data. We therefore asked if the two-site binding model can match the SSPT curves.

To model the case where monomeric actin may have a second binding site, as considered for the case of SC, we define c_wa as the concentration of monomeric actin with this second site bound. We also define c_waw as the concentration of monomeric actin with both sites bound. We then have the

additional equilibrium expressions

$$c_{\mathrm{wa}} = \frac{c_{\mathrm{a}} c_{\mathrm{w}}}{K_{\mathrm{d},2}}, \tag{S7}$$

$$c_{\mathrm{waw}} = \frac{c_{\mathrm{aw}} c_{\mathrm{w}}}{K_{\mathrm{d},12}}. \tag{S8}$$

We consider the case where $K_{\mathrm{df}} \to \infty$ (no incorporation of WH2 domains into filaments). In this case, the mass balances become

$$c_{\mathrm{a}}^0 = K_{\mathrm{da}} \left(\eta + \left(1 + \frac{K_{\mathrm{d}}}{K_{\mathrm{d},2}} \right) \xi + \frac{K_{\mathrm{d}}}{K_{\mathrm{d},12}} \frac{\xi^2}{\eta} + 2 K_2 K_{\mathrm{da}} \eta^2 + 3 K_3 K_{\mathrm{da}}^2 \eta^3 + K_4 K_{\mathrm{da}}^3 \frac{(4 - 3\eta)\eta^4}{(1-\eta)^2} \right), \tag{S9}$$

$$c_{\mathrm{w}}^0 = K_{\mathrm{da}} \left(\frac{K_{\mathrm{d}}}{K_{\mathrm{da}}} \frac{\xi}{\eta} + \left(1 + \frac{K_{\mathrm{d}}}{K_{\mathrm{d},2}} \right) \xi + 2 \frac{K_{\mathrm{d}}}{K_{\mathrm{d},12}} \frac{\xi^2}{\eta} \right), \tag{S10}$$

where

$$\xi \equiv \frac{c_{\mathrm{a}} c_{\mathrm{w}}}{K_{\mathrm{da}} K_{\mathrm{d}}}. \tag{S11}$$

Equation (S10) is quadratic in ξ. We can therefore solve for $\xi(\eta)$ (keeping only the physical root), and can insert this expression into (S9). The resulting equation is solved numerically for $0 < \eta < 1$. Upon solution, we compute

$$f_{\mathrm{fil}} = 1 - \frac{1}{c_{\mathrm{a}}^0} \left(c_{\mathrm{a}} + c_{\mathrm{aw}} + c_{\mathrm{wa}} + c_{\mathrm{waw}} \right) = 1 - \frac{K_{\mathrm{da}}}{c_{\mathrm{a}}^0} \left(\eta + \left(1 + \frac{K_{\mathrm{d}}}{K_{\mathrm{d},2}} \right) \xi + \frac{K_{\mathrm{d}}}{K_{\mathrm{d},12}} \frac{\xi^2}{\eta} \right). \tag{S12}$$

In solving for the SSPT curve, we again take $K_{\mathrm{d},2} \approx K_{\mathrm{d},12}$, as we did in treating the competition anisotropy curves. The results are plotted in Fig. S4D. We see that the two-site model serves to move the corner concentration toward smaller values than the one-site model, and is therefore in contrast to the experimental measurements. We thus conclude that the two-state binding model, in the absence of filament binding, does not describe the SSPT measurements.

Supplementary figures

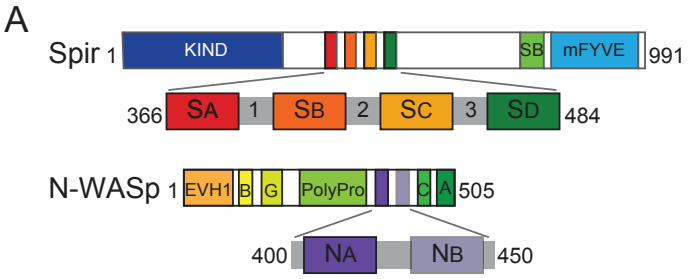

B

Construct name	Amino Acid Sequence
SA	WARFWVQVIDELRRGVRLKKSNHER
SB	GPLGSELTPYEILMGDIRAKKYQLRKVMVNGAAAS
SC	GPLGSKKDAHAMILEFIRSRPPLKKASDRQAAAS
SD	GPLGSEPSPREQLMESIRKGKELKQITPPEAAAS
SD-KCK	GPLGSEPSPREQLMESIRKGKELKQITPPEKCK
NA	GPLGSGNKAALLDQIREGAQLKKASDRQLGAAAS
NA[fs]	GPLGSGNKAALLDFIRSGAQLKKASDRQLGAAAS
SC[qe]	GPLGSKKDAHAMILEQIRERPPLKKASDRQAAAS
SC3	GPLGSKKDAHAMILEFIRSRPPLKKASDRQLGPPRMCEPSHHHHHH
S3D	GPLGSASDRQLGPPRMCEPSPREQLMESIRKGKELKQITPPE
SC3D	GPLGSKKDAHAMILEFIRSRPPLKKASDRQLGPPRMCEPSPREQLMESIRKGKELKQITPPEAAAS
SC3C	GPLGSKKDAHAMILEFIRSRPPLKKASDRQLGPPRMCEPSAHAMILEFIRSRPPLKKASDRQHHHHHH
SD3D	GPLGSEPSPREQLMESIRKGKELKQASDRQLGPPRMCEPSPREQLMESIRKGKELKQITPPEHHHHHH
NAS3D	GPLGSGNKAALLDQIREGAQLKKASDRQLGPPRMCEPSPREQLMESIRKGKELKQITPPEAAAS
NAS3NB	GPLGSGNKAALLDQIREGAQLKKASDRQLGPPRMCEPSGRDALLDQIRQGIQLKSVSDGQAAAS
SD3C	GPLGSEPSPREQLMESIRKGKELKQASDRQLGPPRMCEPSAHAMILEFIRSRPPLKKASDRQHHHHHH
SC3NB	GPLGSKKDAHAMILEFIRSRPPLKKASDRQLGPPRMCEPSGRDALLDQIRQGIQLKSVSDGQAAAS
SC[qe]3D	GPLGSKKDAHAMILEQIRERPPLKKASDRQLGPPRMCEPSPREQLMESIRKGKELKQITPPEAAAS
NA[fs]S3D	GPLGSGNKAALLDFIRSGAQLKKASDRQLGPPRMCEPSPREQLMESIRKGKELKQITPPEAAAS
SC[gs]D	GPLGSKKDAHAMILEFIRSRPPLKKAGSGSGSGSGSCEPSPREQLMESIRKGKELKQITPPEAAAS

Figure S1: Constructs used in this paper. (A) Domain architecture of Spir and N-WASp are shown for reference. Domains are defined in Figure 1. (B) Table includes the names (left) and amino acid sequences (right) of all constructs used. Colored boxes are the WH2 domains. The light grey boxes are Linker 3. Outside of the boxes are residues that remain after GST cleavage (GPLGS), are due to cloning strategy (AAAS), are added for labeling (KCK), or purification (His_6).

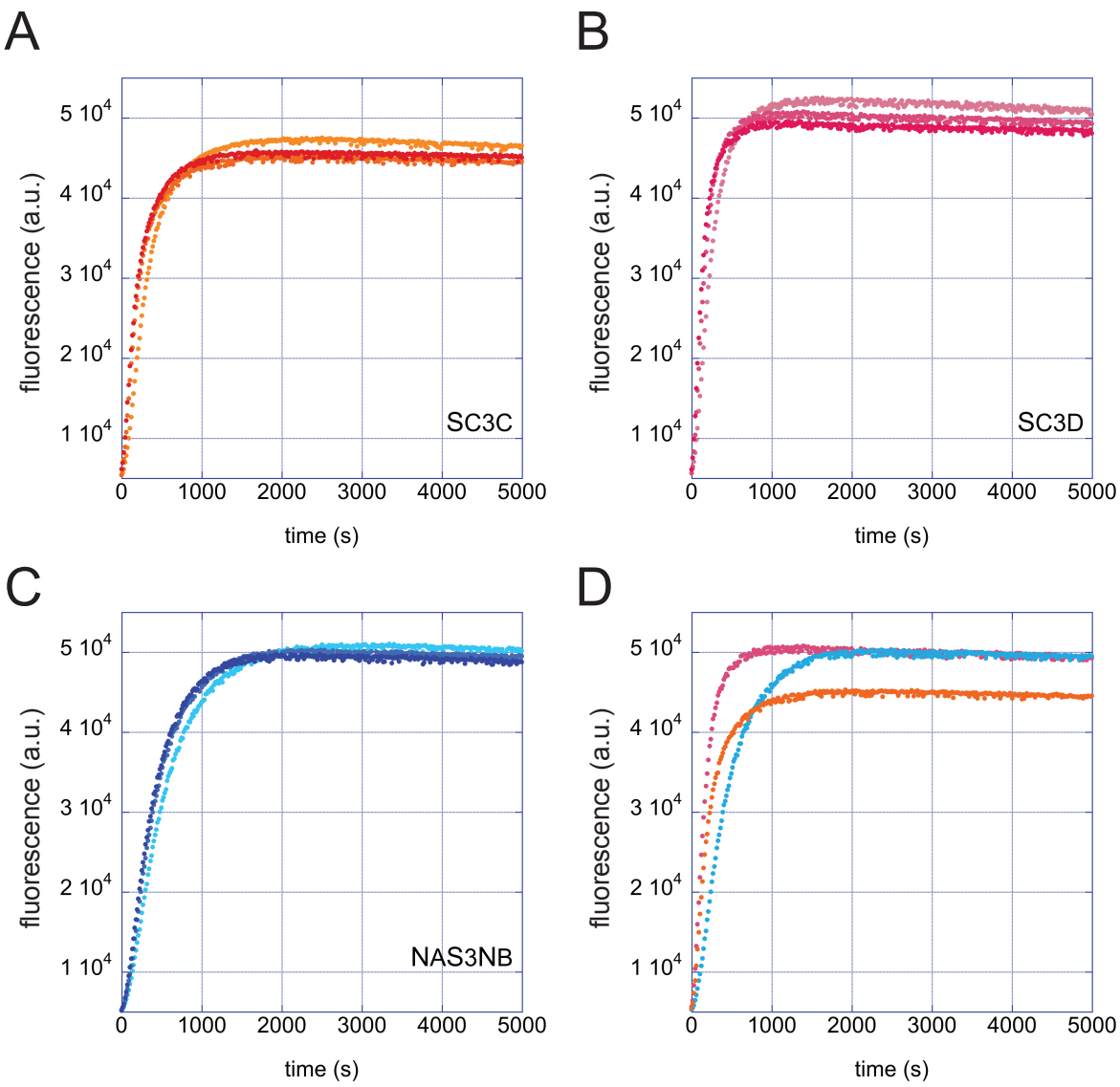

Figure S2: Sequestration analysis. (A-C) Pyrene-actin polymerization assays performed with 4µM actin (5% pyrene) and 250, 500 or 1000 µM (light to dark shades of each color) of the indicated WH2-Linker 3-WH2 construct. (D) Comparison of 500 µM SC3C, SC3D and NAS3NB. The plateau of SC3C is markedly lower than those of the other two constructs at each concentration.

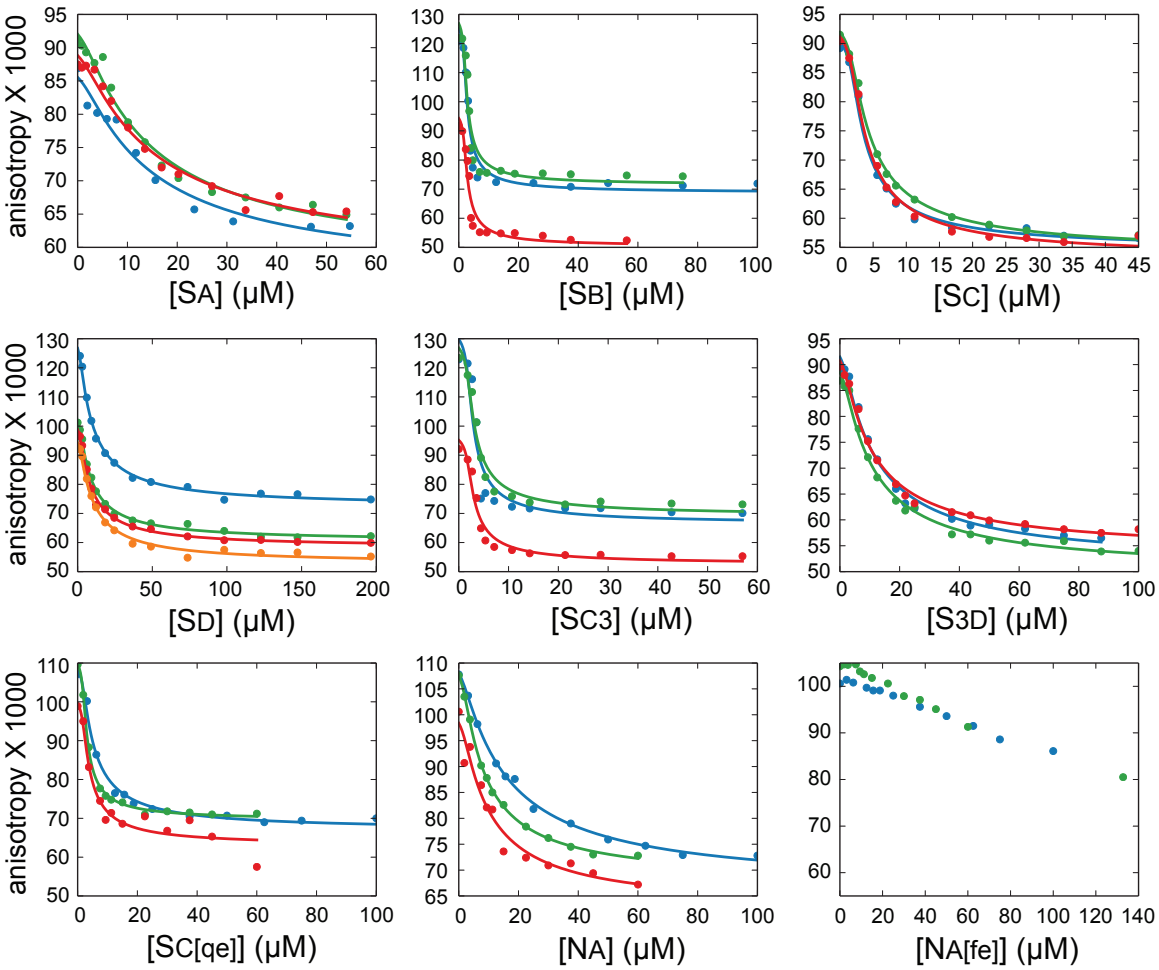

Figure S3: Fluorescence anisotropy experiments of each WH2 domain. Each regression was performed independently. Like colors are regressions of respective data sets. Average affinities from these three trials are reported in Figure 3A and Table 1.

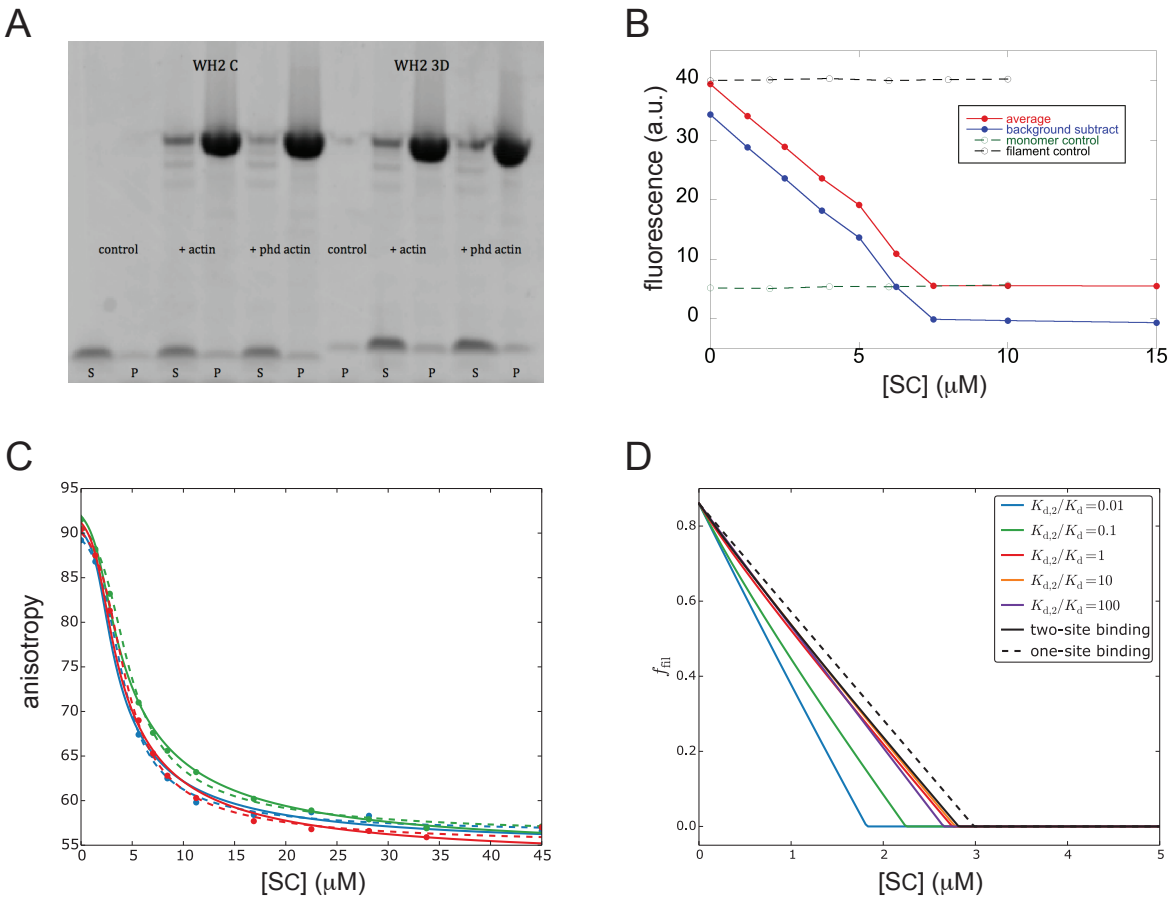

Figure S4: Filament binding controls. (A) Co-sedimentation assay with SCand S3D. 12 μM WH2 domain was used. Controls have no actin. Experiments have 4 μM actin alone (+actin) or in the presence of equimolar phalloidin (+phd). Supernatants (S) and pellets (P) were separated and run on a gel. (B) Latrunculin-actin (monomer control) or phalloidin-actin (filament control) was mixed with increasing concentrations of SCunder the same conditions used in the SSPT assay. In both cases the signal change was less than 1% of that measured in the experiment. The three experimental repeats were averaged and are shown here (red). Monomer and filament controls were used to calculate the background and subtract it from the original data (blue). (C) Competition fluorescence anisotropy titration regressions for SC where we consider alternate stoichiometry. Each color represents an independent titration. All titrations used 5 nM SD* and 2 μM actin. The solid lines use the one-site binding model, where the dashed lines use the two-site binding model. (D) Theoretical SSPT curves. For colored curves, $K_{\mathrm{d}} = 0.21$ μM, as determined from the competition anisotropy experiments under the one-site binding model. The solid black curve results from the best-fit parameters of the two-state model to the competition anisotropy data. The dashed curve results from the best-fit parameters from the one-state binding model.

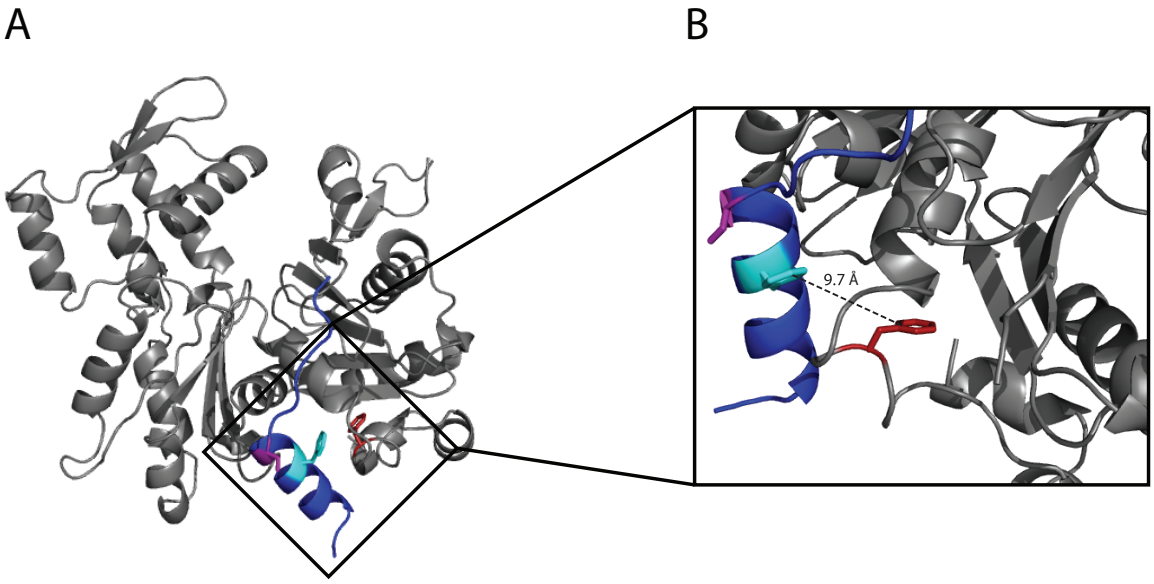

Figure S5: Homology model of SC and actin co-crystal: (A) SC domain (blue) replaces SD in a co-crystal with *A. castellani* actin (grey) pdb: 4EFH. Actin Phe352 (red) is part of an unstructured loop and with minimal rearrangements may stack with SC Phe438 (cyan). Because it is small and uncharged, SC Ser441 (purple) allows for this rearrangement, contributing to the Phe stacking and deeper placement of SCinto the actin hydrophobic pocket. (B) Zoom in box region from (A). The dashed line represents the distance between SC Phe-438 and actin Phe-352.